Glycoconj J (2009) 26:301–311
DOI 10.1007/s10719-008-9166-0

Survey of *O*-GlcNAc level variations in *Xenopus laevis* from oogenesis to early development

Vanessa Dehennaut · Tony Lefebvre · Yves Leroy · Jean-Pierre Vilain · Jean-Claude Michalski · Jean-François Bodart

Received: 10 April 2008 / Revised: 13 June 2008 / Accepted: 20 June 2008 / Published online: 17 July 2008

Abstract Little is known about the impact of *O*-linked-*N*-acetylglucosaminylation (*O*-GlcNAc) in gametes production and developmental processes. Here we investigated changes in *O*-GlcNAc, UDP-GlcNAc and *O*-GlcNAc transferase (OGT) levels in *Xenopus laevis* from oogenesis to embryo hatching. We showed that in comparison to stage VI, stages I–V oocytes expressed higher levels of *O*-GlcNAc correlating changes in OGT expression, but not in UDP-GlcNAc pools. Upon progesterone stimulation, an *O*-GlcNAc level burst occurred during meiotic resumption long before MPF and Mos-Erk2 pathways activations. Finally, we observed high levels of *O*-GlcNAc, UDP-GlcNAc and OGT during segmentation that decreased concomitantly at the onset of gastrulation. Nevertheless, no correlation between the glycosylation, the nucleotide-sugar and the glycosyltransferase was observed after neurulation. Our results show that *O*-GlcNAc is regulated throughout oogenesis and development within a complex pattern and suggest that dysfunctions in the dynamics of this glycosylation could lead to developmental abnormalities.

V. Dehennaut · T. Lefebvre (✉) · Y. Leroy · J.-C. Michalski
UMR-CNRS 8576,
Unité de Glycobiologie Structurale et Fonctionnelle,
IFR 147, USTL,
59655 Villeneuve d'Ascq, France
e-mail: tony.lefebvre@univ-lille1.fr

V. Dehennaut · J.-P. Vilain · J.-F. Bodart
Laboratoire de Régulation des Signaux de Division,
EA4020, IFR 147, USTL,
59655 Villeneuve d'Ascq Cedex, France

J.-F. Bodart
Institut de Recherches Interdisciplinaires CNRS-USR 3078,
groupe des nanosystèmes biologiques, USTL,
59655 Villeneuve d'Ascq cedex, France

Keywords *O*-GlcNAc · OGT · *Xenopus laevis* · Oogenesis · Meiosis · Embryogenesis

Introduction

Cell division, differentiation and migration occurring from oogenesis to early development are intricate processes that are spatially and temporally finely controlled. These processes are orchestrated by many signals brought by post-translational modifications (PTM). Among these PTM, *O*-linked *N*-acetylglucosaminylation (*O*-GlcNAc) has been shown to be crucial in many aspects of the cellular life. Owing to the plethora of the *O*-GlcNAc-modified proteins, deciphering the role of this glycosylation in cell physiology remains a challenge.

O-GlcNAc is a dynamic PTM that can sometimes counteract phosphorylation on a same or on a neighbouring amino-acid. The reversibility of *O*-GlcNAc is managed only, by a pair of enzymes that are highly conserved from *Caenorhabditis elegans* to human. The *O*-GlcNAc transferase (OGT) modifies the target polypeptide chain by adding the *N*-acetylglucosamine group from UDP-GlcNAc [1, 2], while a *N*-acetylglucosaminidase, named *O*-GlcNAcase [3], removes the *O*-GlcNAc moiety. The sugar-nucleotide UDP-GlcNAc is generated through the hexosamine biosynthetic pathway (HBP), whose flux directly depends upon the availability of extracellular glucose. Numerous families of proteins are affected by *O*-GlcNAc, including transcription factors, chaperones, metabolic enzymes, kinases, phosphatases and architectural proteins. Accumulating literature led to consider this PTM as a modulator of a wide variety of cell signalling cascades [4]. Recently, it has been shown that the cellular *O*-GlcNAc content was dynamically modified during the mammalian and the

amphibian cell cycle [5, 6]. In these studies, the authors showed that OGT overexpression lead to multi-nucleation and cytokinesis defect [5] and that OGT activity is requested for G2-M transition in *Xenopus* oocytes [6]. From these different studies, the idea that *O*-GlcNAc could play a pivotal role in the control of cell division has emerged.

Beyond the description of the *O*-GlcNAc functionality during cell division, only a few observations have been so far gathered on the role of *O*-GlcNAc during oogenesis and development. The only data describing *O*-GlcNAc levels during the oogenesis process were obtained by Slawson *et al.* [7]. Stages-I and II oocytes were reported to express more *O*-GlcNAc than stages-III to VI and the decrease in *O*-GlcNAc modification was correlated with an increase in *O*-GlcNAcase activity. Strikingly, only a few studies dealing with *O*-GlcNAc and development have been reported. Knockouts of OGT have been successfully performed in *C. elegans* [8] and in mouse [9, 10]. Knockouts of murine OGT are lethal for embryos and stem cells [10] and preliminary studies on OGT conditional knockouts have induced an early death at day 4 or 5 post-implantation [9]. *C. elegans* ogt-1 and oga-1 knockouts, respectively for OGT and *O*-GlcNAcase, have offered advantageous opportunities to analyse the effects of *O*-GlcNAc content modifications in the insulin-like signalling cascade. Unfortunately, these models did not provide yet clues for a role of these enzymes during early embryogenesis [8, 11], since no differences in the nuclear accumulation of five embryonic temporally and spatially regulated transcription factors (HLH-1, HLH-2, ELT-2, SKN-1 and LIN-26) were observed between wild type, ogt-1 and oga-1 knockouts [8, 11]. On the contrary, it has been reported that the transcriptional variants of OGT found in zebrafish embryos varied at the onset of morphogenetic movements [12], supporting the idea that OGT is regulated during embryogenesis and that it is involved in developmental processes.

Due to their large size, their year-around availability and their ease of manipulation, embryos of *Xenopus* species have become a popular model for studying developmental biology in the last half-century [13]. In anticipation for fertilization, oocytes achieve two distinct biological processes termed oogenesis [14] and oocyte maturation, respectively [15]. During oogenesis and oocytes growth, nutrients and stock maternal mRNAs accumulate according to specific patterns. At the end of oogenesis, fully grown oocytes, or immature oocytes, are arrested in prophase of first meiotic division. Upon hormonal stimulation, oocytes resume meiosis: germinal vesicles break down (GVBD), chromosomes condense and a meiotic spindle is formed, which will enable gametes to proceed for genetic material segregation. Nevertheless, at the end of maturation oocytes are blocked in metaphase of second meiotic division in anticipation for fertilization. This maturation process is dynamically controlled by the M-Phase promoting factor (MPF, Cdk1-Cyclin B) and by the Mos-Erk2 pathways. Fertilization of *Xenopus* eggs initiates a series of rapid and synchronous cell divisions that, within 6 to 7 h, produce a 'sphere', which is called blastula, of approximately 4,000 cells with an internal cavity or blastocoel. Then, morphogenetic movements referred as gastrulation organize the future adult body plan. Thereafter, neurulation begins, which leads to the differentiation and regional organization of the nervous system of the embryo. Numerous studies have precisely described the synchronous cleavages of blastomeres prior to midblastula transition (MBT) [16], and the spatiotemporal patterns of cell division during gastrulation and neurulation [17].

Though OGT has been cloned in *Xenopus* species [*Xenopus* (*Silurana*) *tropicalis*] [18], the patterns of *O*-GlcNAc, OGT and UDP-GlcNAc have not been yet deciphered in amphibians during early embryogenesis. The aim of the present work is to provide a platform to study the *O*-GlcNAc levels in oogenesis, maturation and in the developmental processes like early cell cycles or morphogenetic movements.

Material and methods

Handling of oocytes

Adults *Xenopus* females were purchased from the University of Rennes I (France). After anesthetizing *Xenopus* females by immersion in 1 g l^{-1} MS222 solution (tricaine methane sulfonate; Sandoz), ovarian lobes were surgically removed and placed in ND96 medium (96 mM NaCl, 2 mM KCl, 1.8 mM $CaCl_2$, 1 mM $MgCl_2$, 5 mM HEPES/NaOH, pH 7.5). Stages I to VI oocytes were spotted and taken according to their size and pigmentation [19]. Oocytes were isolated and follicle cells were partially removed by 1 mg ml^{-1} collagenase A (Roche Applied Science) treatment for 30 min followed by a manual microdissection. Oocytes were stored at 14°C in ND96 medium until experiments.

Germinal vesicle breakdown (GVBD) kinetics experiments

Meiotic resumption was induced by incubating stage VI oocytes in ND96 medium containing 10 μM of progesterone (Sigma-Aldrich). All experiments were performed at 19°C. GVBD, which reflects oocyte entry into the maturation process was scored by the appearance of a white spot at the animal pole of the oocyte. For each time point, batches of ten oocytes were taken respecting the white spots ratio and stored at −20°C until biochemical analyses.

Oocyte activation kinetics experiments

Stage VI oocytes were incubated overnight in ND96 medium containing 10 μM of progesterone. The next day, metaphase II-arrested oocytes were transferred into ND96 medium containing 1 μM calcium ionophore (A23187, Sigma-Aldrich). For each time point, batches of 5 activated-oocytes were taken according to morphological criteria (*i.e.*, pigment contraction at the animal pole of the oocyte) and stored at −20°C until biochemical analyses.

In vitro fertilization (IVF)

To obtain eggs, females were primed with 500 U of human chorionic gonadotropin (hCG, Sigma-Aldrich). The male was euthanized, testis were dissected and kept in 0.1X MBS (Modified Barth's Saline, 88 mM NaCl, 1 mM KCl, 1 mM $MgSO_4$, 2.5 mM $NaHCO_3$, 10 mM $CaCl_2$, 5 mM HEPES/NaOH, pH 7.8) medium at 4°C until use. For fertilization, eggs were harvested by squeezing the abdomen of the female, directly transferred into a Petri dish and a fragment of testis was gently "paint" over the surface of the eggs. Ten minutes after fertilization, dishes were flood with 0.1X MBS. Then fertilized eggs were dejellied in 2% (*w*/*v*) cysteine (Sigma-Aldrich) adjusted to pH 8.0 with NaOH, rinsed three times with 1X MBS and replace in 0.1X MBS. Development of embryos was allowed at 23°C. Batches of five embryos were taken at different times of development according to the normal table of *Xenopus laevis* (Daudin) [20] and kept at −20°C for biochemical analyses.

SDS-PAGE and Western blotting

Proteins (the equivalent of one oocyte or one embryo was loaded per lane) were run on a 17.5% modified SDS-PAGE—this kind of gel allows a better discrimination between protein isoforms of phosphorylation-and electro-blotted onto nitrocellulose sheet [21]. Blots were saturated in 5% (*w*/*v*) non-fatty milk in TBS (Tris-buffered saline)-Tween [15 mM Tris/HCl, 140 mM NaCl, 0.05% (*v*/*v*) Tween] for 45 min. Primary antibodies were incubated overnight at 4°C. Mouse monoclonal anti-*O*-GlcNAc (RL-2; Affinity Bioreagents), rabbit polyclonal anti-OGT (DM-17; Sigma-Aldrich), mouse monoclonal anti-Erk2 (D-2; Santa Cruz Biotechnologies), rabbit polyclonal anti-β-catenin (H-102; Santa Cruz Biotechnologies) and rabbit polyclonal anti-Cyclin B2 (generously provided by Dr. John Gannon from the ICRF, South Mimms, UK) antibodies were used at a dilution of 1:1,000. Rabbit polyclonal anti-actin (I-19; Santa Cruz Biotechnologies) antibodies were used at a dilution of 1:10,000. Then nitrocellulose membranes were washed three times for 10 min each in TBS-Tween and incubated with either an anti-mouse horseradish peroxidase-labeled secondary antibody or an anti-rabbit horseradish peroxidase-labeled secondary antibody (GE healthcare) at a dilution of 1:10,000. Finally, three washes of 10 min each were performed with TBS-Tween and the detection was carried out with enhanced chemiluminescence (GE Healthcare).

UDP-GlcNAc pools measurement by HPAEC (high performance anion exchange chromatography)

Oocytes or embryos were lysed in 1 ml of hypotonic buffer (10 mM Tris/HCl, 10 mM NaCl, 15 mM 2-mercaptoethanol, 1 mM $MgCl_2$ and proteases inhibitors, pH 7.2). Fifty microlitres of 1 M HCl were then added to the lysate and the mixture was passed through a 1.5 ml Dowex 50WX2-400 column. The column was washed with 7.5 ml of bi-permuted water (18 MΩ water). The unbound fraction and washes were collected on ice and adjusted to pH 8.0 with 500 μl of Tris/HCl 1 M. Of the diluted fraction, 500 μl was injected using a ProPAC-PA1 column (4×250 mm) on a Dionex (Jouy en Josas, France) HPLC system. The elution was achieved as following: Tris/HCl 20 mM, pH 9.2 (solution A) for 1 min; elution gradient for 29 min with 85% of A and 15% NaCl at 2 M (solution B); plateau of 5 min in the same conditions; 10 min elution gradient until 100% of B was reached; plateau at 100% of B for 5 min. The column was then re-equilibrated in 100% of A. The flow rate was 0.8 ml min^{-1}. Detection was performed using a UV–visible spectrophotometric detector (SPD-6AV, Shimadzu, Champs sur Marne, France) at a wavelength of 256 nm.

Densitometric analyses

Variations of *O*-GlcNAc contents and OGT expression were performed by densitometric analyses of Western Blots using the GeneTools software (File version: 3.07.03; Syngene).

Results

O-GlcNAc, OGT and UDP-GlcNAc contents vary during oogenesis

Stages I-VI oocytes were isolated according to criteria of size and pigmentation (Fig. 1A). After extraction, proteins were resolved by SDS-PAGE and analyzed according to their *O*-GlcNAc content, OGT and β-catenin expression and equal loading of the gel was ascertained by an anti-actin staining (Fig. 1B, representative of four independent experiments). The data of four experiments were summarized in Fig. 1C for the changes in *O*-GlcNAc level and in Fig. 1D for the OGT expression. We observed a high

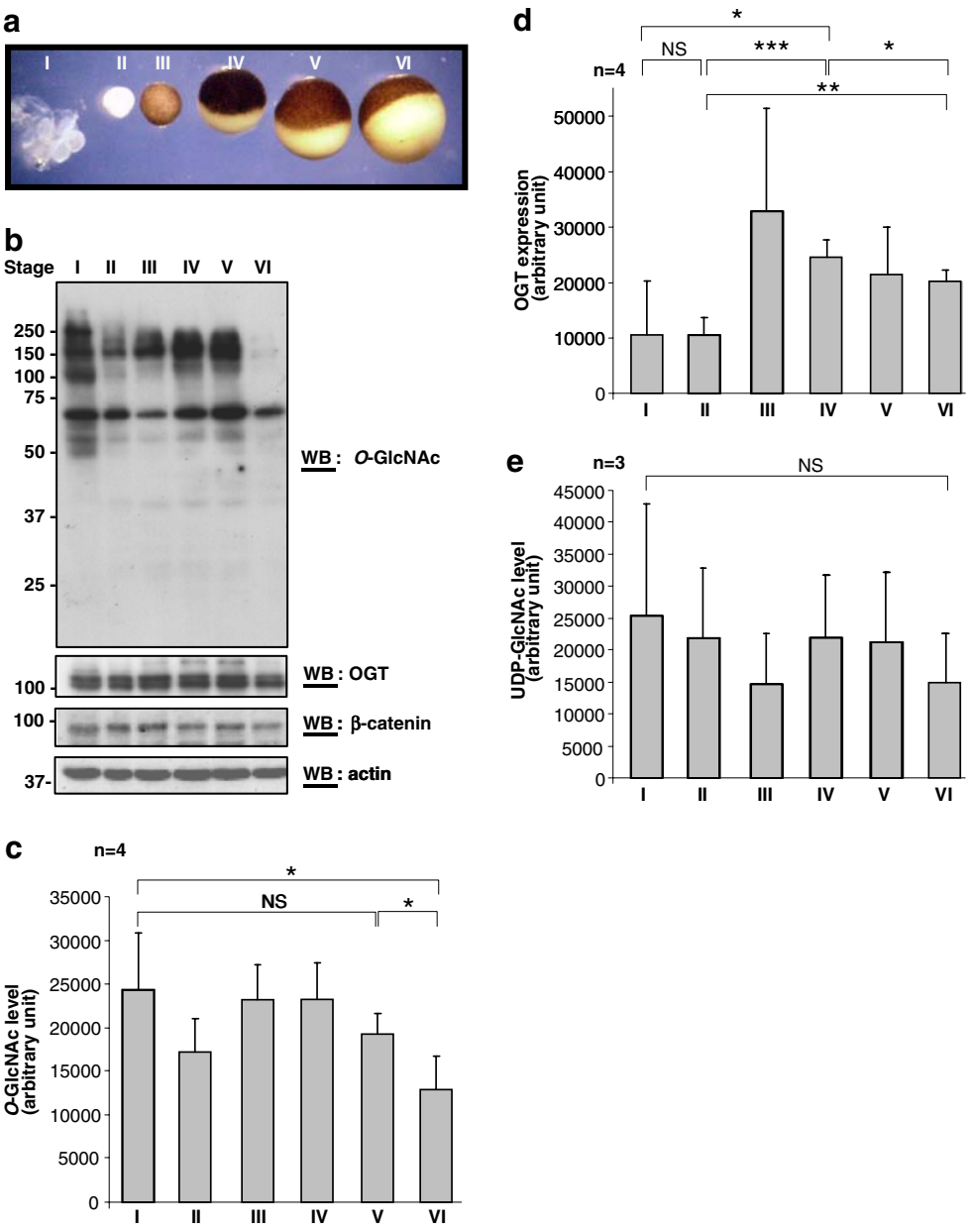

Fig. 1 *O*-GlcNAc content decreases during oogenesis. **A** Pictures showing the time course of oogenesis. Stages I to VI oocytes were taken according to criteria of size and pigmentation [19]. **B**—Oocytes were homogenized in lysis buffer and analysed according to their *O*-GlcNAc, OGT, β-catenin and actin contents by Western blot. Protein mass markers are indicated at the *left* (kDa). *WB* Western blot. **C** Histogram showing the *O*-GlcNAc level obtained by densitometric analyses of Western blots. Results correspond to the mean value± SD of four independent experiments (**P*<0.05, ***P*<0.01, ****P*<0.001, respectively, *NS* not significative). **D** Histogram showing the OGT expression obtained by densitometric analyses of Western blots. Results correspond to the mean value± SD of four independent experiments (**P*<0.05, ***P*<0.01, ****P*<0.001 respectively, *NS* not significative). **E** UDP-GlcNAc pools of the different stages of oocytes were assessed by HPAEC. Results correspond to the mean value±SD of three independent experiments (**P*< 0.05, ***P*<0.01, ****P*<0.001 respectively, *NS* not significative)

and a rather constant *O*-GlcNAc level from stage I to stage V oocytes that was followed by a slight decrease of the glycosylation status at stage VI (Fig. 1B and C). The latter decrease was partially correlated to the slight decrease in OGT expression shown for stage VI oocyte when compared to stages I–IV oocytes (Fig. 1B and D). Note that the OGT expression increase observed between the oocytes of stage II and the oocytes of stage III could not be considered as significant due to the high variability found for the stage III OGT amount from one experiment to another. No change in the β-catenin content was observed. For each stage, the UDP-GlcNAc pool was assayed using high performance anion exchange chromatography (Fig. 1E) as previously described [6]. No significant changes in the UDP-GlcNAc pools were observed between the different stages.

Progesterone-induced meiotic resumption is accompanied by a fast increase in O-GlcNAc content long before the mos-erk2 and the MPF pathways activation

Previously, we reported that *Xenopus* oocyte meiotic resumption was accompanied with a burst in the *O*-GlcNAc content [22], and that OGT inhibition [6] or recombinant OGT microinjection [23] altered the GVBD progression, underlying the crucial role of *O*-GlcNAc in meiotic resumption. To determine the timely occurrence of *O*-

GlcNAc increase during meiosis progression, fully-grown stage VI oocytes (Fig. 2A, left picture) were stimulated with progesterone. Every 2 h post-progesterone addition, oocytes were scored for white spot formation, attesting GVBD (Fig. 2A, right picture). GVBD percentages were calculated and reported in a histogram (Fig. 2B). For each time point, batches of ten oocytes were collected respecting the white spot ratio. The oocytes were lysed and analyzed by Western blot according to their *O*-GlcNAc content and their OGT expression (Fig. 2C, two top panels). Activations of the Mos-Erk2 and MPF pathways were examined using an anti-Erk2 antibody and an anti-Cyclin B2 antibody, respectively (Fig. 2C, two middle panels). The discrimination between the active form and the non active form of these two proteins is based on the doublet pattern of both proteins: the non-phosphorylated lower migrating one is the inactive form, whereas the upper band is the active phosphorylated form. The accumulation of β-catenin and the expression of actin were also examined (Fig. 2C, two bottom panels). The anti-*O*-GlcNAc staining showed a burst of the *O*-GlcNAc level 2 h after the meiotic resumption stimulation: at this time, none of the oocytes exhibited morphological (Fig. 2B) or biochemical (Fig. 2C) typical changes characteristic of GVBD. In this set of experiments, the first white spots appeared only 6 h after progesterone incubation but Erk2 and Cyclin B2 can be detected in their activated form only 8 h after progesterone treatment. This *O*-GlcNAc rise does not seem to be correlated with an increase in OGT expression since we did not observe any changes in OGT level during the time course of the GVBD kinetic. In contrast, β-catenin started to accumulate 6 h post-progesterone treatment and reach a maximal expression near 10 h after hormonal stimulation.

Since the *O*-GlcNAc level increased long before the activation of the Mos-Erk2 and the MPF pathways, we hypothesized that its up-regulation coincides with the early events of meiotic resumption. The two first hours following hormonal stimulation by progesterone, batches of oocytes were taken every 10 min and analyzed as described above (Fig. 2D). Western blots presented in Fig. 2D are representative of four independent experiments. The averages and the standard deviations of the different values obtained for these four independent experiments were calculated and represented in two histograms: Fig. 2E for *O*-GlcNAc changes and Fig. 2F for OGT expression. We observed a statistically significant increase in *O*-GlcNAc content 40 min after progesterone stimulation (Fig. 2D and E). *O*-GlcNAc increased progressively until 80 min and then remained at a constant level. Even if there is no significant difference in OGT expression when we compared time 0 to time 120 min (Fig. 2D and F), slight variations can be detected during this time laps, which are concomitant with the *O*-GlcNAc profile: OGT expression increased between 0 and 90 min and slightly decreased thereafter. These results underline a potential role for *O*-GlcNAc glycosylation in the initiation of the meiotic resumption.

O-GlcNAc level is kept high and constant during oocyte activation

At the end of the maturation process, eggs are arrested at the metaphase of the second meiotic division in anticipation for fertilization. The interaction between the sperm and the egg membrane provokes a rise in the intracellular calcium, which is responsible of egg activation [24]. The calcium wave releases the egg from metaphase II arrest and is characterized by both inactivation of the MPF and the Mos-Erk2 pathways mainly due to Cyclin and Mos proteolysis by the ubiquitin–proteasome pathway [25, 26]. Ca^{2+}-increasing agents mimic the fertilization calcium wave, thereby activating eggs metabolism and ending meiosis. To investigate the *O*-GlcNAc dynamics upon egg activation, metaphase II-arrested oocyte were stimulated with the calcium ionophore A23187. Eggs exhibiting typical morphological sign of activation (pigments contraction at eggs apex; Fig. 3A, right), were taken every 5 min and analyzed according to their *O*-GlcNAc content, OGT expression, β-catenin accumulation as described above (Fig. 3B). Activation process triggering was ensured by checking the Erk2 and the Cyclin B2 status. We observed a degradation of Cyclin B2 15 min post calcium ionophore stimulation followed by a newly synthesis of the protein 30 min after metaphase II released (Fig. 3B, see the arrow heads on the anti-Cyclin B2 staining) and an inactivation of Erk2 30 min post-release. These results are consistent with previous reports [27]. Except slight variations for some *O*-GlcNAc proteins, both *O*-GlcNAc level and OGT expression remained high and constant during the time course of the experiment as well as β-catenin stability. Thus, calcium induced-egg activation is not accompanied with any significant changes in *O*-GlcNAc level or OGT expression.

O-GlcNAc dynamics during early embryogenesis

Next we studied *O*-GlcNAc level changes accompanying *Xenopus* early embryogenesis. After fertilization, embryos were taken off at different stages of the embryogenesis process from the cortical rotation until hatching according to the Normal Table of Daudin (Fig. 4A) [20]. More precisely, the glycosylation levels were examined during early cleavages (Fig. 4A, stages 1–6), late segmentation (Fig. 4A, stages 7–9), gastrulation (Fig. 4A, stages 10–11.5), neurulation (Fig. 4A, stages 12.5–21) and beginning of the organogenesis before (Fig. 4A, stages 22–25) and after the hatching of the embryo (Fig. 4A, stages 25–28).

After lysis of the embryos, proteins were resolved on SDS-PAGE and analyzed according to their *O*-GlcNAc content, OGT expression and β-catenin accumulation (Fig. 4B). β-catenin was used here as a marker for embryogenesis progression. Indeed, as it has been intensively described [28], accumulation of β-catenin was observed along with blastomere cleavages during segmentation process (Fig. 4B, stages 1–9). From gastrulation to hatching, embryos exhibited high amounts of the protein. An accumulation of its fragments of proteolysis were revealed on Western blot as lower migrating bands. The results presented in Fig. 4B are representative of five independent experiments. These different experiments were summarized in Fig. 4C for changes in the *O*-GlcNAc level and in Fig. 4D for the OGT expression. We have also determined the UDP-GlcNAc levels for three independent experiments as described in Fig. 1 (Fig. 4E). From the histograms and Western blots analyses, one can observe that the *O*-GlcNAc level was very high during the early cleavages and the segmentation of the embryos (Fig. 4B and C, stages 1–9). This *O*-GlcNAc rate is correlated with an increasing expression of OGT between stage 1 and 9 (Fig. 4B and D), but also with a slight increasing amount of UDP-GlcNAc (Fig. 4E). At the onset of gastrulation, *O*-GlcNAc, OGT and UDP-GlcNAc significantly dropped. Thereafter, *O*-GlcNAc content continued to diminish until the mid-neurula (Fig. 4C, compare stage 11.5–12 with 15–17), but no correlation was found with the OGT expression (Fig. 4D) and the UDP-GlcNAc level (Fig. 4E), this latter UDP-GlcNAc level staying relatively low until stage 28. Finally, *O*-GlcNAc level only re-increased at the late neurula and remained high even after the hatching of the embryo.

Fig. 2 Progesterone-induced meiotic resumption is accompanied by a fast increase in *O*-GlcNAc content. **A** The *left picture* represents a fully grown stage VI oocyte, namely immature oocyte. Upon progesterone stimulation, immature oocyte resumes meiosis. This phenomenon is first characterized by the germinal vesicle breakdown (*GVBD*), which leads to the appearance of a white spot at the animal pole of the oocyte indicated by WS (*right picture*). **B** Meiotic resumption was induced by progesterone treatment. Every 2 h post-progesterone stimulation, oocytes were observed and white spots corresponding to GVBD oocytes were counted. The histogram shows the percentage of GVBD during the time course of oocyte maturation of one representative experiment. Oocytes were picked up respecting the white spots ratio for further biochemical analyses. **C** For each time point, oocytes were homogenized in lysis buffer and analysed according to their *O*-GlcNAc, OGT, β-catenin and actin contents by Western blot. Activation of the Mos-Erk2 and MPF pathways were also assessed using respectively an anti-Erk2 and an anti-Cyclin B2 antibody. Arrows heads at the right of the figure indicate the phosphorylated (*phospho*) and the non-phosphorylated (*non-phospho*) forms of CyclinB2 and Erk2. Protein mass markers are indicated at the *left* (kDa).*WB* Western blot, *Pg* progesterone. Results are representative of four independent experiments. **D** Stage VI oocytes were stimulated with progesterone and picked up every 10 min until 2 h. During this laps time, no morphological sign of GVBD were observed. A batch of ten GVBD oocytes was also taken 12 h post-progesterone treatment and served as a maturation positive control (*right of the figure*). **O**ocytes were analysed according to their *O*-GlcNAc, OGT and actin contents by Western blots. Protein mass markers are indicated at the *left* (kDa).*WB* Western blot, *Pg* progesterone. **E** Histogram showing the *O*-GlcNAc level obtained by densitometric analyses of Western blots. Results correspond to the mean value±SD of five independent experiments (**P*<0.05, ***P*<0.01, ****P*<0.001 respectively, *NS* not significative). **F** Histogram showing the OGT expression obtained by densitometric analyses of Western blots. Results correspond to the mean value±SD of five independent experiments (**P*<0.05, ***P*<0.01, ****P*<0.001 respectively, *NS* not significative)

Discussion

External development in amphibians and fishes offers the unique opportunity to directly monitor morphological and biochemical events occurring during embryogenesis, related to proliferation, differentiation and migration. In this study we took advantage of the African clawed frog *Xenopus laevis* model to assess the levels of *O*-GlcNAc, UDP-GlcNAc and OGT expression from oogenesis to early embryogenesis.

Among the plethora of PTM regulating signaling pathways, addition and removal of *O*-GlcNAc on target proteins have emerged as a key regulation feature of nuclear and cytoplasmic proteins fates. The functions of *O*-GlcNAc have been partially explored during gametogenesis in the sole model of amphibian [6, 7, 22, 29], but strikingly, this model has not been extensively exploited. Yet a few years ago, the works of Fang and Miller [29] have stressed the potential role of *O*-GlcNAc in the cell cycle progression. These authors have capped *O*-GlcNAc moieties by micro-injecting galactosyltransferase into the cytoplasm of *Xenopus* oocytes, blocking both *O*-GlcNAc removal and *O*-GlcNAc-mediated lectin-like interactions. This approach led to the observation that *O*-GlcNAc removal blockade was toxic for cell cycle progression, especially at the G2/M phase transition; in return it has limited effect in immature oocytes. These results strengthened the importance of *O*-GlcNAcase in the removal of *O*-GlcNAc residues that are necessary for the progression of the cell cycle. Unfortunately, at this moment no antibody raised against the *Xenopus O*-GlcNAcase is available limiting the study of the hydrolase. On the same model, Slawson *et al.* [7] described higher levels of *O*-GlcNAc in stages I–II oocytes in comparison to the stages III–IV, that they correlated to an increase of the *O*-GlcNAcase activity. While for some experiments the anti-*O*-GlcNAc profiles we have obtained were close to the profile reported by these authors, we failed to detect any statistically significant changes between oocytes from stages I to V. Nevertheless, we observed a

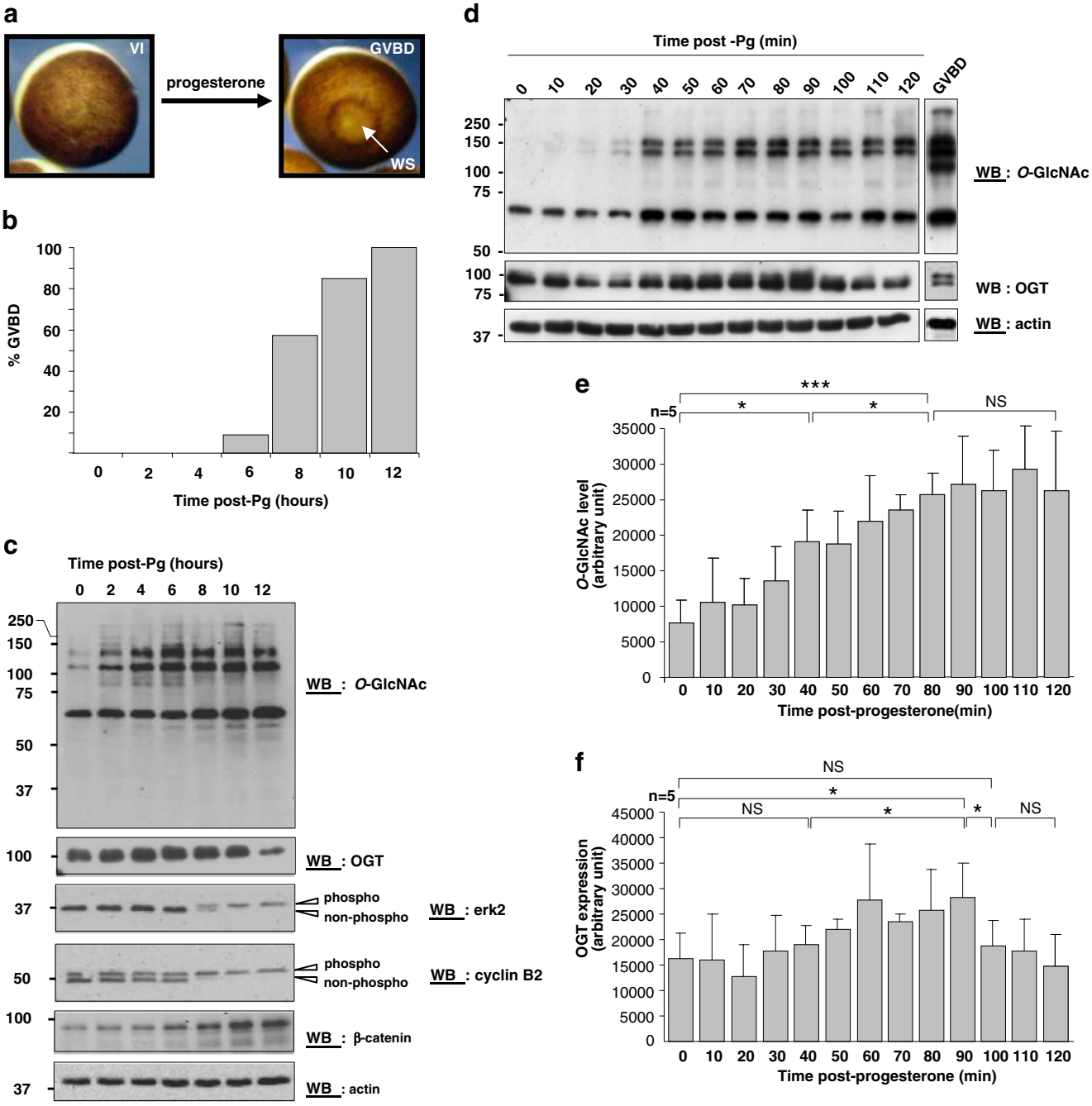

drop in the *O*-GlcNAc level in stage VI compared to stage V. This drop was neither related to a decrease in OGT expression nor in the UDP-GlcNAc levels since both did not exhibit major changes between stages V and VI. This *O*-GlcNAc decrease might be rather related to an increase in the *O*-GlcNAcase activity, as previously proposed [7]. Once oogenesis is achieved, stage VI oocytes resume maturation process upon hormonal stimulation by progesterone. In this context, we previously reported that oocyte GVBD or M-phase entry was accompanied by an increase in *O*-GlcNAc level and that OGT inhibitors prevented meiosis progression. In contrast, inhibiting the HBP rate-limiting enzyme glutamine: fructose-6-phosphate amidotransferase (GFAT) with azaserine or DON, failed to interfere with the GVBD kinetics [6]. The ineffectiveness of these two inhibitors was explained by the assay of the UDP-GlcNAc pools of immature and matured oocytes that revealed that the nucleotide-sugar concentration was unchanged during the meiotic resumption. Thus, oocytes run on a preexisting UDP-GlcNAc pool during GVBD. Since

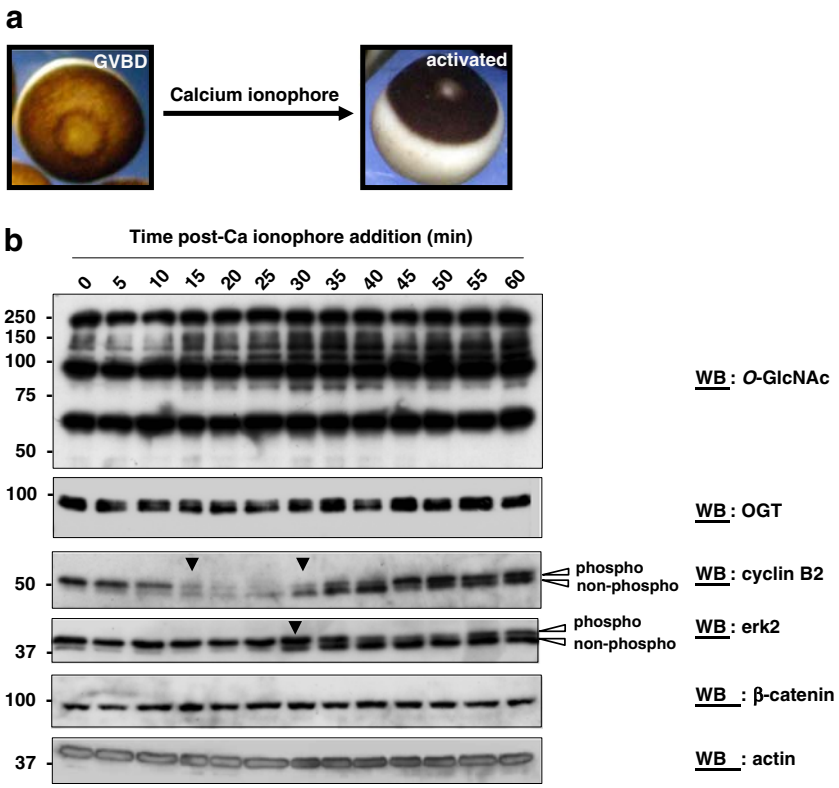

Fig. 3 The *O*-GlcNAc level stays high and constant during oocyte activation. Metaphase II-arrested oocyte activation was stimulated by the calcium ionophore addition. Oocytes which presented morphological sign of activation were taken every 5 min after stimulation until 60 min for biochemical analyses. **A** Pictures showing a metaphase II-arrested oocyte (*left picture*) *versus* an activated one (*right picture*) with typical contracted pigments at the animal pole of the oocyte. **B** For each time point, oocytes were homogenized in lysis buffer and analysed according to their *O*-GlcNAc, OGT, β-catenin and actin contents by Western blots. The level of activity of the Mos-Erk2 and MPF pathways were also assessed using an anti-Erk2 and an anti-cyclin B2 antibody, respectively. *White arrowheads* at the *right* of the figure indicate the phosphorylated (*phospho*) and non-phosphorylated (*non-phospho*) forms of CyclinB2 and Erk2. The *black arrowheads* point out the time of inactivation and the re-synthesis of Cyclin B2 and the inactivation of Erk2. Protein mass markers are indicated at the *left* (kDa). *WB* Western blot

meiotic progression does not depend upon UDP-GlcNAc changes, we further looked at OGT expression during GVBD time course experiments. We observed that the burst in the *O*-GlcNAc level preceded by several hours the activation of both the MPF and the Mos-Erk2 pathways and that this *O*-GlcNAc increase did not correlate with changes in OGT expression. Then, we attempted to determine the precise dynamics of the *O*-GlcNAc variation at the early steps of meiotic resumption. A significant change in *O*-GlcNAc content was observed about 40 to 50 min following progesterone addition, whereas a transient and slight peak of OGT expression was observed. One can hypothesize that this *O*-GlcNAc increase could be linked to the early events of meiotic resumption, one of them being a reduction in cAMP leading to PKA inactivation [30]. PKA has been shown to inhibit GFAT by modifying the Ser205 [31]. Such PKA inhibition could be one way to increase the *O*-GlcNAc levels in oocyte. But as previously discussed, we have demonstrated that the inhibition of

Fig. 4 *O*-GlcNAc level fluctuates all along early embryogenesis. **A** ▶ Pictures representing the different developmental stages according to the Normal Table of *Xenopus laevis* (Daudin) that were analysed in this study. **B** For each developmental stage showed above, embryos were homogenized in lysis buffer and analysed according to their *O*-GlcNAc, OGT, β-catenin and actin contents by Western blots. Results are representative of five independent experiments. **C** Histogram showing the *O*-GlcNAc level obtained by densitometric analyses of Western blots. Results correspond to the mean value±SD of three to five independent experiments (**P*<0.05, ***P*<0.01, ****P*<0.001, respectively, *NS* not significative). **D** Histogram showing the OGT expression obtained by densitometric analyses of Western blots. Results correspond to the mean value±SD of three to five independent experiments (**P*<0.05, ***P*<0.01, ****P*<0.001, respectively, *NS*, not significative). **E**—UDP-GlcNAc pools of the different stages of oocytes were assessed by HPAEC. Results correspond to the mean value±SD of three independent experiments (**P*<0.05, ***P*<0.01, ****P*<0.001, respectively, *NS* not significative)

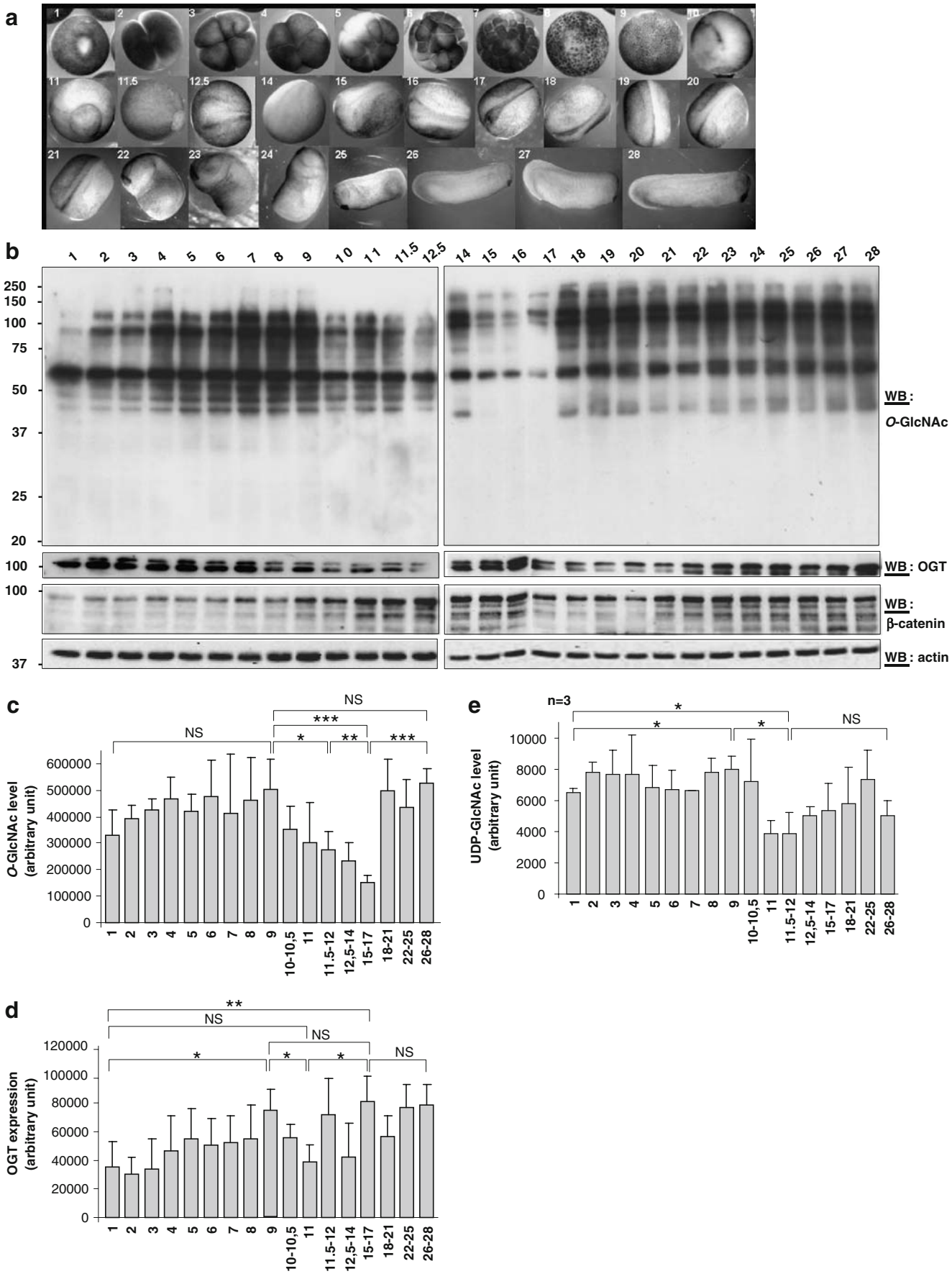
a
b
WB: O-GlcNAc
WB: OGT
WB: β-catenin
WB: actin
c
O-GlcNAc level (arbitrary unit)
d
OGT expression (arbitrary unit)
e
n=3
UDP-GlcNAc level (arbitrary unit)
NS
10-10,5
11.5-12
12,5-14
15-17
18-21
22-25
26-28

GFAT was inefficient in our attempts to block the meiotic resumption [6]. Another event occurring within the first hours following hormonal stimulation is the activation of the poly-adenylation machinery, which permits the translation of key-proteins like Mos and Cyclin B [32, 33]. Even if only a few papers described the implication of *O*-GlcNAc in the translational processes, the hypothesis that *O*-GlcNAc would control both the poly-adenylation and/or the translation machinery should not be not discarded [34].

From fertilization to early organogenesis, three successive phases may be discriminate correlatively to *O*-GlcNAc, UDP-GlcNAc levels and OGT expression: (1) from fertilization to the onset of gastrulation, (2) from gastrulation to the beginning of closure of the neural tube (stage 15–17) and finally (3) from stage 17 up to stage 28. β-catenin, which is essential for the dorsal determination of *Xenopus* embryos [28, 35], was used in our set of experiments as a marker for embryogenesis progression. β-catenin does not accumulate in immature oocytes while being phosphorylated by GSK-3β and then degraded; its accumulation appeared to be dependent upon *O*-GlcNAc [22]. Because both GSK-3β and β-catenin are substrates for OGT [22, 36], a role for OGT in the accumulation of the dorsal determinant of the embryo is hypothesised. Here we observed that UDP-GlcNAc and *O*-GlcNAc levels remained high during segmentation, which is consistent with an active role for *O*-GlcNAc in proliferation and cell cycle regulation mechanisms [4–6, 23]. Interestingly, we observed a decrease of *O*-GlcNAc content and a decrease in OGT expression at the onset of gastrulation, a step at which cytoskeletal arrangements driven by rapid cell divisions are not compatible with those needed for morphogenesis [37]. If inhibitory phosphorylation of MPF is considered as a key regulation to postpone mitosis to favor gastrulation, down-regulation of *O*-GlcNAc levels might also emerge as a key event for morphogenetic movements at gastrulation. Concomitantly to *O*-GlcNAc level and OGT expression decreases, we observed a drop in the UDP-GlcNAc pool. This drop might be due to the beginning of glycolysis, starting at the onset of gastrulation [38, 39]. Indeed, once entered into the cell, glucose is immediately phosphorylated into glucose-6-phosphate that in turn is isomerized into fructose-6-phosphate. This latter could then either enter the glycolysis to produce ATP or could be directed through the HBP for forming UDP-GlcNAc. The ATP production is crucial for cell migration, which requests cell shape rearrangements: the drop in *O*-GlcNAc level observed at the onset of gastrulation could be then driven by the need of glucose to produce energy. A role for *O*-GlcNAc variation in development has been also suspected in the zebrafish [12], in which six variants for zOGT (var1-6) were found and shown to be regulated at the mRNA level during embryogenesis: var1 and 2 mRNAs disappeared at the shield stage, whereas var3 and 4 mRNA were reported to increase at this stage, where the morphogenetic movements of epiboly begins. mRNAs levels of var5 and 6 remained quite constant throughout the embryogenesis. Unfortunately, no *O*-GlcNAc activity measurements have been performed in this model that would have given an insight in the role of this shift of zOGT expression at the onset of gastrulation. While mechanisms underlying the morphogenetic movements may differ from zebrafish to amphibian, both models suggest a role for *O*-GlcNAc regulating enzymes at the onset of gastrulation.

Finally, an increase in *O*-GlcNAc was observed at the beginning of the neural tube closure (stage 17), correlated with an increase in UDP-GlcNAc, while no significant changes in OGT expression were found from stage 17 to 28. Further works are requested to determine the localization of OGT, as well as *O*-GlcNAcase, since *O*-GlcNAc levels, OGT and *O*-GlcNAcase expressions may exhibit organ-specific patterns. Special attention may be focused on neural tissues, since *O*-GlcNAc is highly expressed in such tissues and that perturbations in this glycosylation have been linked to neurodegenerative disorders [40].

This study provides a platform to decipher the functions of *O*-GlcNAc in the developmental processes and suggest unsuspected and specific functions for *O*-GlcNAc regulating proteins during embryonic events like cell migration occurring especially during gastrulation or cell differentiation associated with organogenesis.

Acknowledgements This work was granted by the "Centre National de la Recherche Scientifique", the "Association pour la Recherche contre le Cancer" and the "Université des Sciences et Technologie de Lille I". We thank Arlette Lescuyer-Rousseau for technical assistance. VD is a recipient of a fellowship from the "Ministère de la Recherche et de l'Enseignement".

References

1. Roos, M.D., Hanover, J.A.: Structure of *O*-linked GlcNAc transferase: mediator of glycan-dependent signaling. Biochem. Biophys. Res. Commun. **271**, 275–280 (2000). doi:10.1006/bbrc.2000.2600
2. Iyer, S.P., Hart, G.W.: Dynamic nuclear and cytoplasmic glycosylation: enzymes of *O*-GlcNAc cycling. Biochemistry. **42**, 2493–2499 (2003). doi:10.1021/bi020685a
3. Lehman, D.M., Fu, D.J., Freeman, A.B., Hunt, K.J., Leach, R.J., Johnson-Pais, T., *et al.*: A single nucleotide polymorphism in MGEA5 encoding *O*-GlcNAc-selective *N*-acetyl-beta-D glucosaminidase is associated with type 2 diabetes in Mexican Americans. Diabetes. **54**, 1214–1221 (2005). doi:10.2337/diabetes.54.4.1214
4. Zachara, N.E., Hart, G.W.: Cell signaling, the essential role of *O*-GlcNAc!. Biochim. Biophys. Acta. **1761**, 599–617 (2006)
5. Slawson, C., Zachara, N.E., Vosseller, K., Cheung, W.D., Lane, M. D., Hart, G.W.: Perturbations in *O*-linked beta-*N*-acetylglucosamine protein modification cause severe defects in mitotic progression and cytokinesis. J. Biol. Chem. **280**, 32944–32956 (2005). doi:10.1074/jbc.M503396200
6. Dehennaut, V., Lefebvre, T., Sellier, C., Leroy, Y., Gross, B., Walker, S., *et al.*: *O*-linked *N*-acetylglucosaminyltransferase inhibition pre-

vents G2/M transition in *Xenopus laevis* oocytes. J. Biol. Chem. **282**, 12527–12536 (2007). doi:10.1074/jbc.M700444200
7. Slawson, C., Shafii, S., Amburgey, J., Potter, R.: Characterization of the *O*-GlcNAc protein modification in *Xenopus laevis* oocyte during oogenesis and progesterone-stimulated maturation. Biochim. Biophys. Acta **1573**, 121–129 (2002)
8. Hanover, J.A., Forsythe, M.E., Hennessey, P.T., Brodigan, T.M., Love, D.C., Ashwell, G., *et al*.: *Caenorhabditis elegans* model of insulin resistance: altered macronutrient storage and dauer formation in an OGT-1 knockout. Proc. Natl. Acad. Sci. U. S. A. **102**, 11266–11271 (2005). doi:10.1073/pnas.0408771102
9. O'Donnell, N., Zachara, N.E., Hart, G.W., Marth, J.D.: Ogt-dependent X-chromosome-linked protein glycosylation is a requisite modification in somatic cell function and embryo viability. Mol. Cell. Biol. **24**, 1680–1690 (2004). doi:10.1128/MCB.24.4.1680-1690.2004
10. Shafi, R., Iyer, S.P., Ellies, L.G., O'Donnell, N., Marek, K.W., Chui, D., *et al*.: The *O*-GlcNAc transferase gene resides on the X chromosome and is essential for embryonic stem cell viability and mouse ontogeny. Proc. Natl. Acad. Sci. USA. **97**, 5735–5739 (2000). doi:10.1073/pnas.100471497
11. Forsythe, M.E., Love, D.C., Lazarus, B.D., Kim, E.J., Prinz, W. A., Ashwell, G.: *Caenorhabditis elegans* ortholog of a diabetes susceptibility locus: oga-1 (O-GlcNAcase) knockout impacts *O*-GlcNAc cycling, metabolism, and dauer. Proc. Natl. Acad. Sci. U. S. A. **103**, 11952–11957 (2006). doi:10.1073/pnas.0601931103
12. Sohn, K.C., Do, S.I.: Transcriptional regulation and *O*-GlcNAcylation activity of zebrafish OGT during embryogenesis. Biochem. Biophys. Res. Commun. **337**, 256–263 (2005). doi:10.1016/j.bbrc.2005.09.049
13. Gurdon, J.B., Hopwood, N.: The introduction of *Xenopus laevis* into developmental biology: of empire, pregnancy testing and ribosomal genes. Int. J. Dev. Biol. **44**, 43–50 (2000)
14. Matova, N., Cooley, L.: Comparative aspects of animal oogenesis. Dev. Biol. **231**, 291–320 (2001). doi:10.1006/dbio.2000.0120
15. Jessus, C., Ozon, R.: How does Xenopus oocyte acquire its competence to undergo meiotic maturation? Biol. Cell. **96**, 187–192 (2004). doi:10.1016/j.biolcel.2003.12.007
16. Masui, Y., Wang, P.: Cell cycle transition in early embryonic development of *Xenopus laevis*. Biol. Cell **90**, 537–548 (1998). doi:10.1016/S0248-4900(99)80011-2
17. Saka, Y., Smith, J.C.: Spatial and temporal patterns of cell division during early *Xenopus* embryogenesis. Dev. Biol. **229**, 307–318 (2001). doi:10.1006/dbio.2000.0101
18. Klein, S.L., Strausberg, R.L., Wagner, L., Pontius, J., Clifton, S. W., Richardson, P.: Genetic and genomic tools for *Xenopus* research: the NIH *Xenopus* initiative. Dev. Dyn. **225**, 384–391 (2002). doi:10.1002/dvdy.10174
19. Dumont, J.N.: Oogenesis in *Xenopus laevis* (Daudin). I. Stages of oocyte development in laboratory maintained animals. J. Morphol. **136**, 153–179 (1972). doi:10.1002/jmor.1051360203
20. Nieuwkoop, P.D. and Faber, J. (Eds): Normal table of *Xenopus laevis* (Daudin). Garland Punlishing, New York (1994).
21. Bodart, J.F., Baert, F.Y., Sellier, C., Duesbery, N.S., Flament, S., Vilain, J.P.: Differential roles of p39Mos-Xp42Mpk1 cascade proteins on Raf1 phosphorylation and spindle morphogenesis in Xenopus oocytes. Dev. Biol. **283**, 373–383 (2005). doi:10.1016/j.ydbio.2005.04.031
22. Lefebvre, T., Baert, F., Bodart, J.F., Flament, S., Michalski, J.C., Vilain, J.P.: Modulation of *O*-GlcNAc glycosylation during Xenopus oocyte maturation. J. Cell. Biochem. **93**, 999–1010 (2004). doi:10.1002/jcb.20242
23. Dehennaut, V., Hanoulle, X., Bodart, J.F., Vilain, J.P., Michalski, J.C., Landrieu, I.: Microinjection of recombinant *O*-GlcNAc transferase potentiates Xenopus oocytes M-phase entry. Biochem. Biophys. Res. Commun. **369**, 539–546 (2008). doi:10.1016/j.bbrc.2008.02.063
24. Sato, K., Fukami, Y., Stith, B.J.: Signal transduction pathways leading to Ca^{2+} release in a vertebrate model system: lessons from Xenopus eggs. Semin. Cell Dev. Biol. **17**, 285–292 (2006). doi:10.1016/j.semcdb.2006.02.008
25. Glotzer, M., Murray, A.W., Kirschner, M.W.: Cyclin is degraded by the ubiquitin pathway. Nature. **349**, 132–138 (1991). doi:10.1038/349132a0
26. Nishizawa, M., Furuno, N., Okazaki, K., Tanaka, H., Ogawa, Y., Sagata, N.: Degradation of Mos by the N-terminal proline (Pro2)-dependent ubiquitin pathway on fertilization of Xenopus eggs: possible significance of natural selection for Pro2 in Mos. EMBO J. **12**, 4021–4027 (1993)
27. Bodart, J.F., Bechard, D., Bertout, M., Gannon, J., Rousseau, A., Vilain, J.P.: Activation of Xenopus eggs by the kinase inhibitor 6-DMAP suggests a differential regulation of cyclin B and p39(mos) proteolysis. Exp. Cell Res. **253**, 413–421 (1999). doi:10.1006/excr.1999.4662
28. Miller, J.R., Moon, R.T.: Signal transduction through beta-catenin and specification of cell fate during embryogenesis. Genes Dev. **10**, 2527–2539 (1996). doi:10.1101/gad.10.20.2527
29. Fang, B., Miller, M.W.: Use of galactosyltransferase to assess the biological function of *O*-linked *N*-acetyl-*d*-glucosamine: a potential role for *O*-GlcNAc during cell division. Exp. Cell Res. **263**, 243–253 (2001). doi:10.1006/excr.2000.5110
30. Wang, J., Liu, X.J.: Progesterone inhibits protein kinase A (PKA) in Xenopus oocytes: demonstration of endogenous PKA activities using an expressed substrate. J. Cell Sci. **117**, 5107–5116 (2004). doi:10.1242/jcs.01383
31. Chang, Q., Su, K., Baker, J.R., Yang, X., Paterson, A.J., Kudlow, J.E.: Phosphorylation of human glutamine:fructose-6-phosphate amidotransferase by cAMP-dependent protein kinase at serine 205 blocks the enzyme activity. J. Biol. Chem. **275**, 21981–21987 (2000). doi:10.1074/jbc.M001049200
32. Sheets, M.D., Wu, M., Wickens, M.: Polyadenylation of c-mos mRNA as a control point in Xenopus meiotic maturation. Nature **374**, 511–516 (1995). doi:10.1038/374511a0
33. Radford, H.E., Meijer, H.A., de Moor, C.H.: Translational control by cytoplasmic polyadenylation in Xenopus oocytes. Biochim. Biophys. Acta **1779**, 217–229 (2008)
34. Datta, B., Ray, M.K., Chakrabarti, D., Wylie, D.E., Gupta, N.K.: Glycosylation of eukaryotic peptide chain initiation factor 2 (eIF-2)-associated 67-kDa polypeptide (p67) and its possible role in the inhibition of the eIF-2 kinase-catalyzed phosphorylation of the eIF-2 alpha subunit. J. Biol. Chem. **264**, 20620–20624 (1989)
35. Heasman, J., Crawford, A., Goldstone, K., Garner-Hamrick, P., Gumbiner, B., McCrea, P., *et al*.: Overexpression of cadherins and underexpression of beta-catenin inhibit dorsal mesoderm induction in early Xenopus embryos. Cell **79**, 791–803 (1994). doi:10.1016/0092-8674(94)90069-8
36. Lubas, W.A., Hanover, J.A.: Functional expression of *O*-linked GlcNAc transferase. Domain structure and substrate specificity. J. Biol. Chem. **275**, 10983–10988 (2000). doi:10.1074/jbc.275.15.10983
37. Duncan, T., Su, T.T.: Embryogenesis: coordinating cell division with gastrulation. Curr. Biol. **14**, R305–R307 (2004). doi:10.1016/j.cub.2004.03.050
38. Dworkin, M.B., Dworkin-Rastl, E.: Metabolic regulation during early frog development: glycogenic flux in Xenopus oocytes, eggs, and embryos. Dev. Biol. **132**, 512–523 (1989). doi:10.1016/0012-1606(89)90246-7
39. Dworkin, M.B., Dworkin-Rastl, E.: Glycogen breakdown in cleaving Xenopus embryos is limited by ADP. Mol. Reprod. Dev. **32**, 354–362 (1992). doi:10.1002/mrd.1080320408
40. Lefebvre, T., Guinez, C., Dehennaut, V., Beseme-Dekeyser, O., Morelle, W., Michalski, J.C.: Does *O*-GlcNAc play a role in neurodegenerative diseases? Expert Rev. Proteomics. **2**, 265–275 (2005). doi:10.1586/14789450.2.2.265